Performance Improvement of a Liquid Propellant Pulsed Plasma Thruster

IEPC-2005-69

Presented at the 29th International Electric Propulsion Conference, Princeton University, October 31 – November 4, 2005

Hiroyuki KOIZUMI*, Yoko KAWAZOE†, Kimiya KOMURASAKI‡, and Yoshihiro ARAKAWA§.
University of Tokyo, Tokyo, 113-8656, Japan

Abstract: A liquid propellant pulsed plasma thruster is a pulsed plasma thruster using liquid as the propellant, especially water is promised as an attractive propellant. In hits work, to increase the thrust to power ratio of a liquid propellant pulsed plasma thruster, seeding additives into water propellant and enhancement of liquid vaporization by a microheater were investigated. Thrust to power ratio of pulsed plasma thrusters is determined by the total resistance of a discharge circuit. Thus the two methods increasing electrical conductivity of plasma were proposed and the experiments were conducted. Sodium chloride was seeded into water, and, as a result, thrust was increased 5 % due to the decrease of the plasma resistance. On the other hand, by enhancing evaporation rate of water using a microheater, the thrust to power ratio was increased up to 8.0 μNs/J, over 30 % in comparison with the previous result. The thruster utilizes two capacitors for the ignition and acceleration, that is double discharge type. The mass shot of 6 μg initiated the main discharge was accomplished without a spark plug. The specific impulse of 1550 s and the trust performance of 6.0 % were attained. From these experimental results, it is shown that high plasma resistance associated with a liquid propellant pulsed plasma thruster using a spark plug causes the low interelectrode pressure.

Nomenclature

C	=	conductance for rarefied gas stream
d	=	distance between electrodes
E	=	capacitor stored energy
I_{bit}	=	Impulse bit
J	=	discharge current
l	=	length of an electrode
L	=	inductance
L'	=	inductance per unit length
m	=	particle mass
T	=	temperature
t	=	time or thickness of an electrode
R	=	resistance or gas constant
R_{plasma}	=	resistance of plasma

* Research associate, Department of Aeronautics and Astronautics, koizumi@al.t.u-tokyo.ac.jp
† Graduate student, Department of Aeronautics and Astronautics.
‡ Associate professor, Department of Advanced Energy.
§ Professor, Department of Aeronautics and Astronautics.

R_{EM} = effective resistance of electromagnetic work
$R_{circuit}$ = resistance of an external circuit, including a capacitor
R_{total} = total resistance of a PPT electrical circuit
w = width of an electrode
λ = heat penetration depth
κ = thermal diffusivity
k = thermal conductivity
ρ = density
τ = current lasting time
C_p = specific heat

I. Introduction

Pulsed Plasma Thrusters (PPTs) have attracted great attention as promising thrusters in recent years.[1] PPTs are pulsed electric propulsion providing high specific impulse in low power levels, whereas most electric propulsions require high power levels. Power throttling of PPTs is managed simply by adjusting the pulse repetition frequency with no influence on the performance. These characteristics are suitable for orbit raising and acquisition of the power limited microspacecraft. In addition, PPTs can generate small impulse bit, and arbitrary impulse is also achieved by adjusting pulse repetition. Hence PPTs are attractive for the accurate positioning, attitude control, and stationkeeping.

To date, the most common PPTs are the Ablative PPTs (APPTs) which use solid propellant. Discharge current flows in a plasma adjacent to the surface of solid propellant. The solid surface is ablated by the current, and supplies the ablated gas as working gas into the plasma. The only moving part is a spring that passively feeds the propellant. Hence APPTs have a very simple structure which provides high reliability, and they are suitable for microspacecraft.

However, APPTs have several problems: 1)poor performance, 2)contamination, 3)nonuniform ablation. 1) For instance, a flight-qualified APPT design had an efficiency of about 8 %.[2] Several researchers in this field have pointed out that the excessive propellant feed which does not contribute to the thrust is the cause of the low efficiency. Low speed vapor continues to be provided from the solid propellant surface after the main discharge,[3,4] because the surface temperature remains higher than the boiling point of the propellant. Additionally the emission of large particulates was observed[5], which could not be effectively accelerated. In order to improve the propellant efficiency, it is necessary to supply only an minimum amount of propellant for both ionization and acceleration. 2) Contamination on the spacecraft by the exhaust gas would become a serious problem, since most APPTs use Teflon® for the propellant, which includes carbon and fluorine. The carbonization was observed on the ignitor plug,[6] and it limited the lifetime of thrusters. Attempts to use alternative polymer propellant failed due to the severe carbonization.[7] Strong reactive elements like fluorine would be serious problems, especially for applications involving sensitive diagnostics like optics on the future spacecraft, although there has not been a research that the contamination did affect spacecraft. 3) The nonuniformity of current density and Teflon surface temperature conducts the preferential ablation near the electrodes.[8] The nonuniform ablation varies the impulse bit trend in successive operation. Further it decreases the amount of usable propellant, and specific impulse in the thruster. This phenomenon was remarkable for the small energy levels and small size.[9,10] Then it would be problem for use as microthruster.

In order to overcome those problems associated with ablative PPTs, we have proposed using liquid as the propellant,[11,12] referred as a liquid propellant pulsed plasma thruster (LP-PPT). It supplies liquid propellant using an intermittent injector into interelectrode space. Especially, water has been focused as promising liquid propellant. It would reduce spacecraft contamination on the sensitive devices of spacecraft and have an advantage capable sharing with other systems like life support system.

In our past study, successful operation of LP-PPT using water as the propellant and its high specific impulse and thrust efficiency were shown.[13,14] The high specific impulse, more than 3000 s, was achieved by throttling the mass shot and not supplying excessive propellant. The thrust to power ratio, however, had remained at lower value than Ablative PPTs. It causes mainly high plasma resistance using water as the propellant. The high plasma resistance was indicated by other liquid propellant PPT researchers also.

In this study, to reduce the high plasma resistance of LP-PPT and increase the thrust to power ratio, we have investigated an effect of seeding additives into water and enhancement of water evaporation using microheater. The former is to increase fractional ionization of plasma by seeding some easily-ionize material in water, and the latter is

to increase total number density of water between electrodes by using microheater to enhance the evaporation of water.

II. Liquid Propellant Pulsed Plasma Thruster

A. Liquid Propellant Pulsed Plasma Thruster

Figure **1** shows the conceptual diagram of LP-PPT. Liquid propellant and injector are installed instead of ablative material (generally Teflon). The liquid injector intermittently injects liquid droplets into interelectrode space. The mass shot, ejected liquid per one operation of the injector, ranged 3 to 50 μg. Breakdown between electrodes is initiated with pressure increase from the liquid or with pre-discharge from a spark plug. The discharge converts liquid and gaseous propellant into plasma. The plasma is accelerated both electromagnetically and electrothermally, and exhausted out of the thruster. Other types of PPT using a liquid propellant were also proposed.[15,16] They supply liquid (water) by allowing diffuse through a porous material with constant mass flow rate.

In Table **1**, the performance of LP-PPT obtained in our past study was shown. Essentially, the impulse per one shot, impulse bit: I_{bit}, was proportional to the capacitor stored energy. Thus thrust to power ratio was almost constant against energy, although there was a little increasing tendency. These are typical characteristics of PPTs, not only LP-PPT. Secondly, impulse bit did not depend the mass ejected from an injector, mass shot. Thus specific impulse and thrust efficiency were inversely proportional to the mass shot. It is different from APPTs, since mass shot of APPTs is proportional to the energy. In our previous study, high specific impulse of 3400 s was achieved by throttling the mass shot.

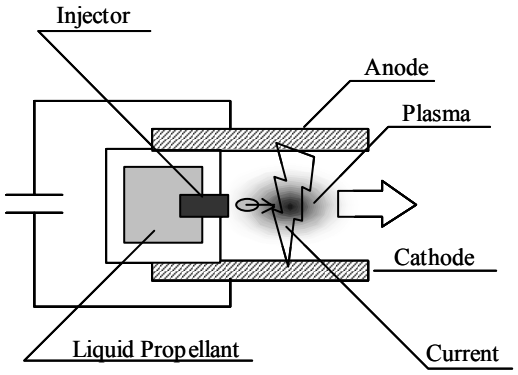

Figure 1. Conceptual diagram of liquid propellant pulsed plasma thruster.

Table 1 Obtained performance of a LP-PPT

Capacitor stored energy	13.5 J
Mass shot	2.8 μg
Propellant	water
Thrust to Power ratio	6.3 μNs/J
Specific Impulse	3400 s
Thrust Efficiency	11 %

B. Electromagnetic Acceleration of a PPT

Generally, a PPT can be assumed as an electrical circuit which has discrete elements of varying inductance, capacitance, and resistance.[17] Electromagnetic impulse that the thruster generates (the momentum given to the plasma by electromagnetic acceleration) is expressed as

$$I_{\mathrm{EM}} = \frac{1}{2} L' \int_0^{\tau} J^2 dt = \frac{1}{2} L' \frac{E}{R_{\mathrm{total}}} \tag{1}$$

where L' is the inductance per unit length, J is the current, E is the capacitor-stored energy, and R_{total} is the total resistance of a PPT. The total resistance consists of the resistance of the external circuit R_{circuit} (capacitor, electrodes, and feed lines), the resistance of the plasma R_{plasma}, and the effective resistance of electromagnetic work R_{EM}.

$$R_{\mathrm{total}} = R_{\mathrm{circuit}} + R_{\mathrm{plasma}} + R_{\mathrm{EM}} \tag{2}$$

Here we assume that the resistances R_{plasma} and R_{EM} are approximately constant during the discharge, although they are actually time varying. Equation (1) means that the small total resistance gives high thrust to power ratio and the impulse generated from electromagnetic accelerator is essentially no dependence on the mass.

C. Comparison between a LP-PPT and an Ablative PPT

Table **2** shows the thrust to power ratios and resistances of a LP-PPT and an Ablative PPT, which were operated by using the same electrodes, electrical feed lines, and a capacitor. Figure **2** shows the configuration of those PPTs with parallel plate electrodes. The measurement methods of thrust and resistance will be explained in the following section **III.C.** and **III.D.**

The liquid propellant PPT had the total resistance of 64 mΩ whereas the ablative PPT with the same configuration had only 48 mΩ as shown in Table **2**. For the LP-PPT , the effective resistance of electromagnetic work was estimated as 10 mΩ from the images taken by a high-speed camera.[18] Hence the plasma resistance of the LP-PPT was about 37 mΩ. It is clearly larger than the plasma resistance of the ablative PPT.

Table 2 Typical resistances of a LP-PPT and Teflon PPT at the energy of 10 J

	LP-PPT	Ablative PPT
Thrust to Power ratio	5.6 μNs/J	8.4 μNs/J
R_{total}	64±2 mΩ	48±1 mΩ
$R_{circuit}$	17±3 mΩ	17±3 mΩ
R_{plasma} + R_{EM}	47±5 mΩ	31±4 mΩ

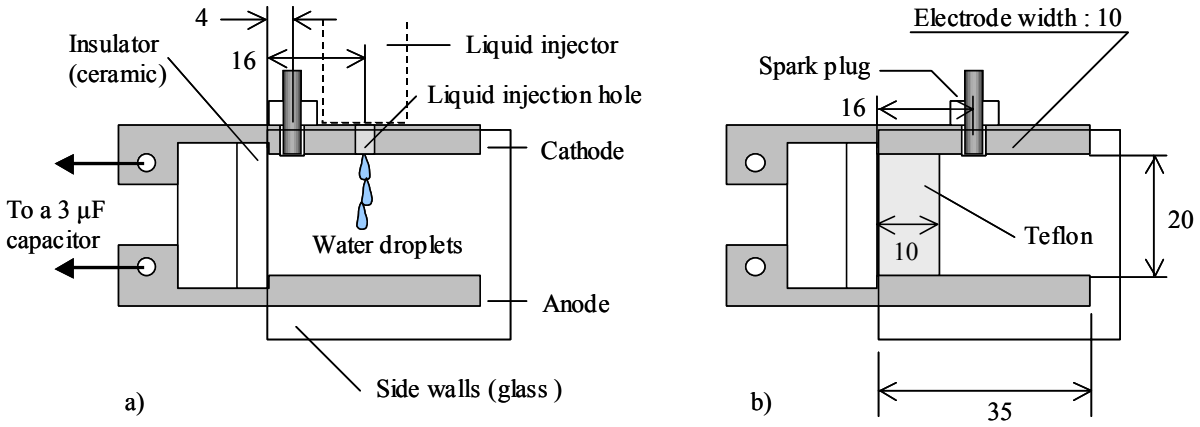

Figure 2. Schematic drawings of PPTs.
a) LP-PPT and b) Ablative PPT.

III. Methods to Decrease the Plasma Resistance

In this study, to decrease the plasma resistance of LP-PPT, the following two methods were investigated.

A. Seeding in Water Propellant

One of the methods to reduce the plasma resistance by increasing fractional ionization is seeding, injecting additives which ionize at relatively low temperatures into the plasma.[19] The additives are ionized in lower temperature than main species, and they supply electron which needs for the ionization of main species.

Here, sodium and ammonia were selected as seeding materials to liquid propellant, water. Table **3** shows the ionization potential of water, sodium, and ammonia and the seed concentration to water by mole percent. The requirement for a good seeding material is low ionization potential, and sodium satisfies that condition. However, injection of sodium as gas state has practical complexities. Thus sodium was seeded into water as sodium chloride aqueous solution due to its handling abilities. In that case, on the other hand, there was no confirmation that sodium was supplied as sodium atom not as crystal of NaCl or something. Then ammonia was selected as a second seeding material as a state of ammonia aqueous solution. Ammonia has lower ionization potential than water, although not as low as sodium. It would be supplied as gas state.

Table 3 Properties of H_2O, Na, and NH_3.

	Ionization potential	Seeding concentration
H_2O	12.7 eV ($\rightarrow H_2O^+$)	-
Na	5.1 eV ($\rightarrow Na^+$)	1.9 %
NH_3	5.9 eV ($\rightarrow NH_3^+$)	5.5 %

B. Enhancement of Vaporization by a Heater

1. Estimation of water droplets evaporation

High resistance of a water propellant PPT can be caused by the total number density in interelectrode space. It would be not liquid droplets themselves but the evaporated gas which directly contributes to plasma. Here, evaporation rate of liquid droplets in a LP-PPT are estimated. There are the following evaporation processes of ejected liquid in LP-PPT: evaporation of flying liquid droplets by it self heat capacity and evaporation of liquid adhering on walls by heat conduction from the walls. Only the evaporated gas contributes plasma and can be utilized as propellant.

Droplets ejected into the vacuum evaporate by themselves heat. The evaporation mass flux: Γ_m is expressed as

$$\Gamma_m = \sqrt{\frac{M}{2\pi RT}} P_{vapor}(T) \tag{3}$$

where P_{vapor} is the vapor pressure at the temperature of liquid. Here the return from the vicinity is neglected. Generally vapor pressure has large dependence on the temperature as shown in Fig. **3**. and that evaporation is suppressed by decrease of temperature due to its latent heat.

For instance, the water droplets of 5 μg has the total surface area of 1.2 mm^2 provided that all droplets have the same diameter of 25 μm. They has the evaporation rate of 3.0 μg/ms at 293 K and 0.4 μg/ms at 263 K. Then flying droplets is rapidly cooled and the evaporation is almost stopped. According to the calculation, only 20 % of the mass will be evaporated within 5 ms and the most is evaporated within 0.5 ms.

Droplets adhering on wall can obtain heat from the wall and keep to evaporate. In this case, the characteristic time of evaporation is determined by the heat conduction inside the walls and droplets. Especially, the heat penetration depth: λ defined by the following equation is useful for evaluation.

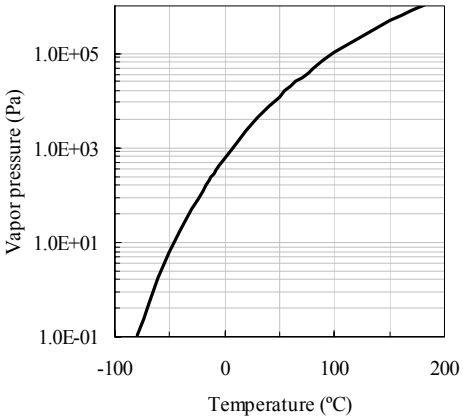

Figure 3. Vapor pressure dependence of water on temperature.

$$\lambda = \sqrt{\kappa t} \tag{4}$$

where κ is the thermal diffusivity and t is the time period. Table **4** shows the thermal properties of water, ethanol, SUS, copper, photoveel, and alumina. Assuming the energy required to vaporize droplets: E_{vaporize} is supplied from the wall by decreasing the temperature ΔT, that energy is roughly estimated as

$$E_{vaporize} = C_p \Delta T \rho \sqrt{\kappa t}^3 \tag{5}$$

For instance, if wall material is copper and the temperature drop is 30 K, vaporization of 5μg of water requires 11 mJ of the energy, 0.5 mm^3 of the volume, and 2 ms. On the other hand, in the case of stainless steel plate, the time is

Table 4 Thermal properties of several materials.

	Water	Ethanol	SUS	Copper	Photoveel*	Alumina
Thermal diffusivity (m^2/s): κ	1.3E-07	8.5E-08	4.0E-06	1.2E-04	5.3E-07	1.1E-05
Thermal conductivity (W/m K): k	0.56	0.17	16	400	1.7	34
Specific heat (J/kg K): C_p	4200	2480	499	380	1218	800
Density (kg/m^3): ρ	1000	785	7920	8920	2590	3930
Heat depth at t = 4 ms (μm): λ	23	18	130	690	50	210

* machinable ceramics produced by SUMIKIN CERAMICS & QUARTZ co.,ltd

extended to 320 ms. It is much longer than the scale of gas escaping from the electrodes, and the pressure rise between electrodes becomes a little.

2. Enhancement of liquid vaporization by a heater

To increase the pressure, namely total number density, between electrodes the at the discharge, we have proposed injecting liquid droplets on a microheater. Pressure between the electrodes is determined by the evaporation rate, not by total mass shot, because the time scale that gas is filled in interelectrode space is less than 0.5 ms in our electrode configuration. The droplets adhering on solid surface are more rapidly vaporized than flying in the vacuum, and its rate depends on the temperature of the solid. Thus, by making liquid adhere on heated surface, the interelectrode pressure would be raised.

The enhancement of vaporization rate by using heater would give two benefits: increase of the interelectrode pressure and breakdown by that pressure increase. The former is to decrease plasma resistance and increase the thrust to power ratio as abovementioned. The latter means spark-plug-less PPT by the breakdown according to the Paschen's low. High voltage sparks of a spark plug cause electromagnetic interference.

The requirements for the heater vaporizing liquid droplets are small heat capacity, high thermal isolation, and high thermal diffusivity of the liquid-adhering-surface. The energy to raise a heater up to the operation temperature should be small in comparison with the capacitor stored energy. However, high thermal isolation of a heater from other parts advantages the continuous operation of PPTs, even if the heat capacity is large. The surface on which liquid droplets adhere should have high thermal diffusivity to quickly conduct the energy to the droplets.

IV. Experimental Facilities and Methods

A. Vacuum Facilities

All of the operation of PPTs were performed in a 1.0-m-diam, 1.4-m-long vacuum chamber. The chamber is evacuated by a turbo molecular pump of the 400 L/s. The base pressures were under 5×10^{-5} Torr through the operation of PPTs.

B. Thrusters

1. Liquid injector

Figure **4** shows the schematic drawing of the liquid injector used through this work. The injector injects liquid from an orifice with the diameter of 25 or 50 μm by its inner pressure. In the closing state (normally state), the force of a spring presses the push rod downward to the orifice. Sealing is achieved by flexible silicone rubber membrane. The rod is pulled upwards by an actuator force. Thus the valve is opened, and inner liquid is ejected by the inner pressure. Liquid is supplied from the feed line beside the main body as not shown in Fig. **4**. There was no pressurization device, and the inside of the liquid tank would ranged from the atmosphere to the vapor pressure of water.

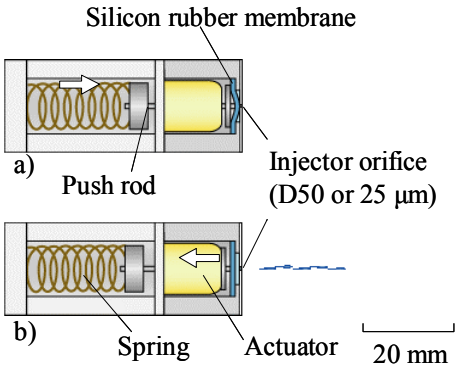

Figure 4. Liquid injector; normally close and intermittent operation. *a) close state and b) open state.*

Figure **5** shows the images of liquid droplets ejected from the liquid injector in the vacuum chamber. The pictures were sequentially taken by every one millisecond by using a of 1000 f/s CCD camera and arc strobe light. Fig. **5** (a) is the ejection using the orifice of 50 μm and Fig. **5** (b) is for

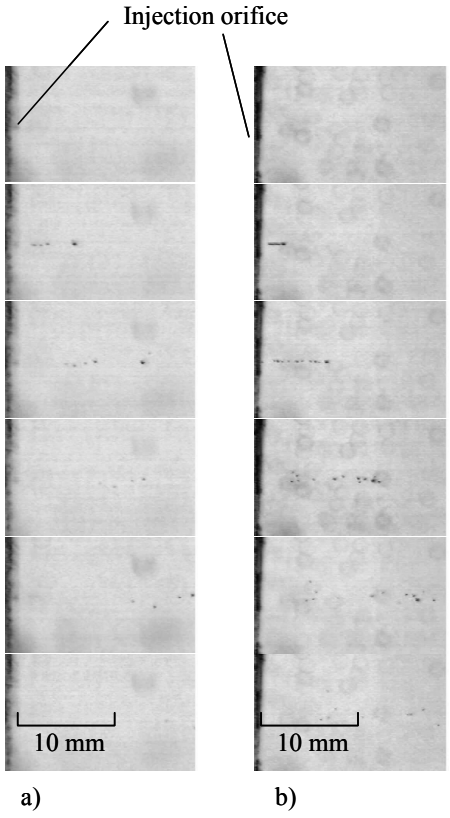

Figure 5. Images of water droplets ejected from the injector orifice, sequentially taken every one millisecond. *a) Orifice diameter:50 μm and b) Orifice diameter: 25 μm.*

the orifice of 25 μm. In the both cases, the mass shot was 5.5 μg.

2. *LP-PPT for the investigation of seeding*

A LP-PPT with parallel plate electrodes shown in Fig. **2** (a) was used in the investigation of seeding effect. The electrodes are parallel plates with 20 mm of the interelectrode distance, 34 mm of the length, and 10 mm of the width. The electrodes are connected to a 3 μF capacitor not shown in the figure. The liquid injector was installed on the cathode. The liquid droplets were vertically supplied through the hole 3mm in diameter opened on the cathode. The liquid injection hole was 16 mm away from the back wall. An spark plug was installed 4 mm away from the back wall.

3. *Microheater assembly*

A commercially available microheater was used to provide the heated solid surface to the liquid droplets. It consists of platinum thin film photoithographically structured on a 0.15 mm thick alumina substrate. The microheater was bound on a copper main body by Torr Seal with a thermocouple lines. The main body consists of a circular plate with 0.8 mm thickness and 4.3 mm diameter and a rectangular plate with 4.3 mm width, 11mm length, 0.6 mm thickness. Liquid droplets is ejected toward the surface of the circular plate. The copper body was surrounded by photoveel shell. The glued component, a microheater, copper main body, thermocouple lines, and photoveel shell, is referred as a microheater assembly. Only the top of the ceramic shell is fixed to an electrode, to avoid the electrical coupling to electrode and insulate from the electrode.

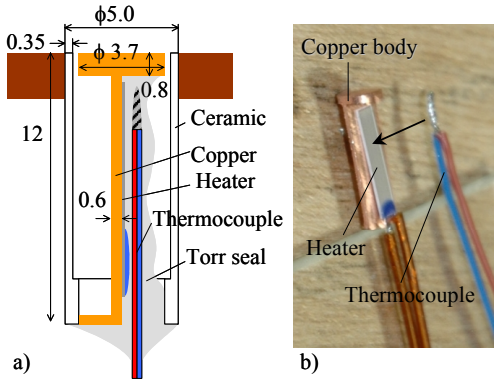

Figure 6. Microheater assembly.
a) schematic drawing of a microheater assembly and b) photograph before the gluing.

Temperature of the microheater was controlled to remain constant by a set point controller. The temperature was ranged from 20 to 100 ˚C. The maximum temperature was restricted by the temperature limit of the glue dealt here, Torr Seal.

4. *LP-PPT for the investigation of enhancement of evaporation using microheater.*

Two varieties of LP-PPTs were designed to enhance the vaporization rate of liquid droplets by the microheater assembly as shown in Fig. **7**. Both LP-PPTs have no spark plug and initiate discharge by breakdown by raising the interelectrode pressure. The first is referred as single discharge LP-PPT and the second is referred as double discharge LP-PPT.

The first, single discharge LP-PPT, has two parts of parallel plate electrodes as shown in Fig. **7** (a): ignition part and acceleration part. Ignition part has the interelectrode distance of 1 mm and the length of 12 mm. Following the ignition part, acceleration part has the electrodes of 20 mm electrode distance and 35 mm length (cathode is 57 mm). These electrodes are made of copper plates with the thickness of 2 mm.

Ignition part is designed to

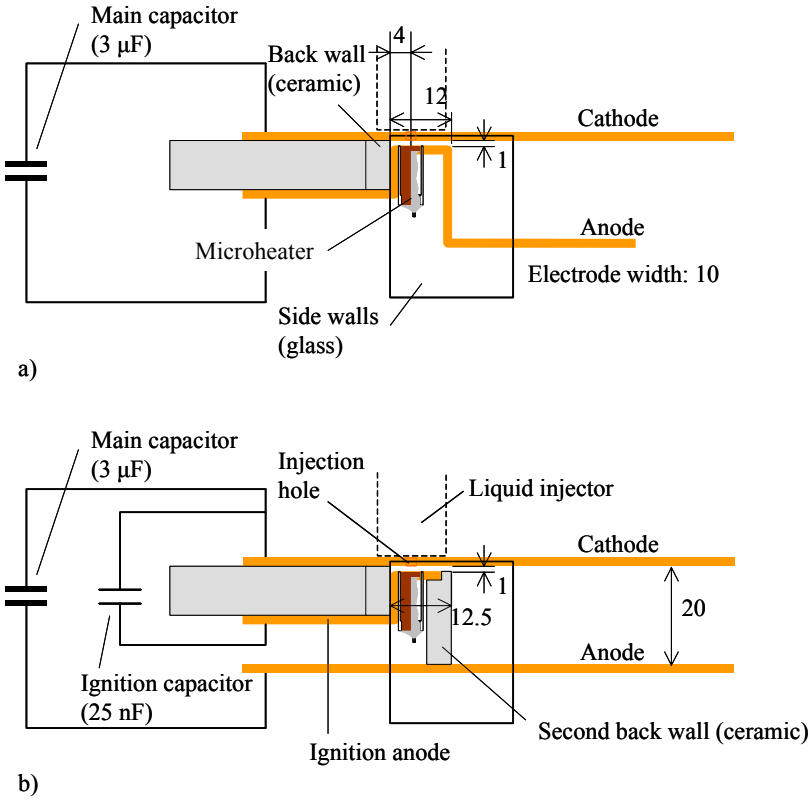

Figure 7. LP-PPT using microheater evaporation.
a) single discharge LP-PPT and b) double discharge LP-PPT.

effectively raise interelectrode pressure. The microheater assembly is installed 4 mm away from the back wall on the anode. Injection hole for liquid droplets was aligned along the center of the receive plate of the microheater. The ejected liquid droplets certainly hit on the plate because of the short interelectrode distance. Moreover the short distance decreases conductance of the channel. Thin parallel plates channel has the following conductance for rarefied gas stream.

$$C = 116 \ln(l/d) \frac{wd^2}{l} \quad (\mathrm{m}^3/\mathrm{s}) \qquad \text{for} \quad l/d > 10 \tag{6}$$

where d is the distance between the plates, l is the length, and w is the width. Therefore the electrode distance quadratically decreases the conductance.

Acceleration part is designed to effectively accelerate the plasma by electromagnetic force. The inductance per unit length: L' for a rectangle circuit with parallel plates is expressed as[20]

$$L' = 0.6 + 0.4 \ln\left(\frac{d}{w+t}\right) \qquad (\mathrm{nH/mm}) \tag{7}$$

where t is the thickness of the plate. The acceleration electrodes have L' of 0.8 nH/mm calculated according to the Eq. (7). For the ignition part, Eq. (7) cannot be applied. Instead,

$$L' = \mu_0 \frac{d}{w} \qquad (\mathrm{nH/mm}) \tag{8}$$

can be applied in the ideal two-dimensional case. Thus ignition part has the L' of 0.13 nH/mm.

The second, double discharge LP-PPT, has two capacitors as shown in Fig. **7** (b): main capacitor of 3 μF and ignition capacitor of 25 nF. Whereas it has two parts as well as the single discharge LP-PPT, anodes of those parts are electrically separated and respectively connected to the capacitors. This design is motivated to prevent the energy to be consumed in the ignition part. Because the ignition part has lower L' than typical PPTs, discharge current passing there hardly contributes to the acceleration. Small discharge plasma generated in ignition part induces main discharge between main electrodes. Hence the ignition part behaves similar to a spark plug. The advantages over a spark plug are that there is no need of high voltage required for a spark plug and that the breakdown occurs automatically when the pressure reaches up to the certain value, which means no necessary of synchronizing the ignition.

Another benefit of the double discharge LP-PPT is to change the capacitor stored energy. The single discharge LP-PPT requires high voltage enough to make breakdown. Therefore there is a restriction to the capacitor stored energy for a fixed capacitance. Nevertheless, in the double discharge LP-PPT, the voltage of the main capacitor can be set under the breakdown voltage, and only the ignition capacitor requires it. Thus the capacitor stored energy can be widely ranged from low level. In this study, 3.0 kV is constantly applied to the ignition capacitor and the voltage applied to the main capacitance is ranged from 1.5 to 3.0 kV.

C. Thrust Measurement

Impulse bits generated by single shot operations of PPTs were measured using a thrust stand,[21] which is a horizontally swinging torsional balance with a 40-cm-long arm. A thruster was installed on the arm of the thrust stand and the reaction force of the thrust was measured in terms of the displacement of the arm. An electromagnetic dumper was to dissipate undesirable vibration of the balance induced by the background mechanical noise. The dumper was turned off before firing of PPT, and the vibration of the balance without

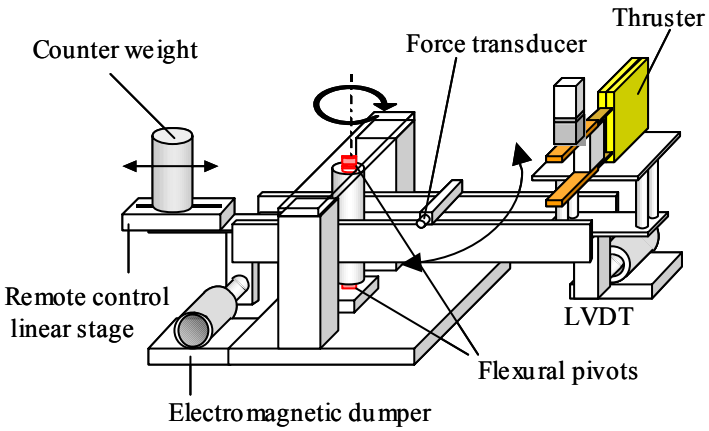

Figure 8. Schematic drawing of thrust stand.

dumping was measured. Counter weights were adjusted to make the gravity center of the balance on the rotation axis, and make the balance stable against the background vibrations. The position of counter weights was finely adjusted by remote control stage in the atmosphere.

Calibration of the thrust stand was performed by striking a force transducer attached to the thrust stand with impact pendulum. The resolution of the thrust stand measurement was ±1.0 μNs and the accuracy of the calibration was ±2%.

D. Resistance Measurement

Resistances of a PPT circuit were measured from a current waveform during a PPT firing. The current was measured using a Rogowski coil installed around a feed line to the capacitor from the capacitor.

1. Total resistance

The total resistance R_{total} was measured by two methods: curve-fit or integral of squared current. In the former method, a current waveform was fit into the following equation.

$$J(t) = J_0 \exp(-\mu t)\sin(\omega t), \quad \text{where} \quad \mu = R/2L \quad \text{and} \quad \omega = \sqrt{1/\text{LC} - \left(\text{R}/2\text{L}\right)^2} \tag{9}$$

This equation consists provided that all the discrete element, L, R, and C were constant during the discharge. This assumption is reasonable in most cases, because the changes of resistance and inductance due to the plasma are not large in comparison with those of the external circuit in typical PPTs. In the latter method, the resistance was determined by the equation

$$R_{total} = E \Big/ \int_0^\tau J^2 dt = \int_0^\tau \left(R_{\text{circuit}} + R_{\text{plasma}} + R_{\text{EM}}\right) J^2 dt \Big/ \int_0^\tau J^2 dt \tag{10}$$

This resistance means squared-current-averaged resistance.

2. Resistance of external circuit

The resistance of the external circuit R_{circuit} was obtained from a current waveform when the electrodes were shorted by a copper plate in the atmosphere. The resistance of the copper plate was less than 0.3 mΩ and negligible. The resistance of the spark generated between the electrode and copper plate was estimated by measuring voltage drop over that spark.

E. Emission Spectroscopy

To confirm the presence of seeding material in the plasma, emission spectroscopy was conducted. The spectrometer dealt here (Hamamatsu; model C5094) has the focal length of 250 mm and 1200 gr/mm grating yielding the reciprocal linear dispersion of 2.5 nm/mm. The dispersed light is detected by a 1024 ch ICCD array. The spectrogram had no resolution in space and time. The emission from the discharge was collected into an optical fiber (not focused), and the exposure time was set as much longer (2 s) than the PPT discharge. The typical slit width was 100 μm. The spectrogram was scanned in 30 nm increments from 320 to 780 nm. The spectral wavelength, and radiance was calibrated using an argon discharge tube and a standard source.

V. Experimental Result

A. NaCl and NH_3 Seeding

Figure **9** shows the dependence of measured thrust to power ratio on the capacitor-stored energy for three types of liquid propellants: purified water, sodium

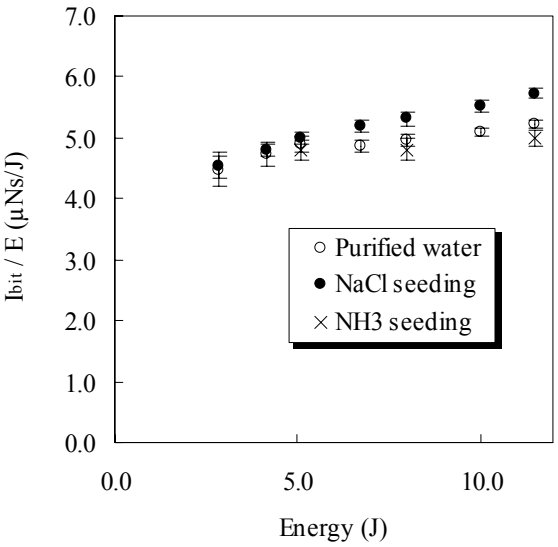

Figure 9. Effect of seeding on the thrust to power ratio of the LP-PPT.

chloride aqueous solution, and ammonia aqueous solution. Capacitor-stored energy was varied from 2.9 to 11.5 J. Every plot of impulse/energy was averaged over 20 or 12 shots. The error bars show the associated standard deviation.

Sodium chloride aqueous solution propellant showed higher thrust power ratio than using purified water. At the energy of 11.5 J, it increases from 60 to 66 μNs, 10 % increase. The average increment of impulse was 5.5 % over the measured energy range. On the other hand, ammonia aqueous propellant showed lower performance.

Figure **10** shows the dependence of total resistance of a liquid propellant PPT on the energy, which is obtained from the curve-fit of the current waveform. The plots mean average over 20 or 12 shots and error bars mean the associated standard deviations. Sodium chloride aqueous propellant showed smaller resistance than purified water, whose average decrement was 5.8 %. Ammonia aqueous solution had larger resistance than purified water had.

Figure **11** shows emission spectrogram from the discharge plasma when sodium chloride aqueous solution and ammonia aqueous solution were used as the propellant. In both cases, liquid propellant PPT was operated for capacitor-stored energy of 11.5 J. As shown in Fig. **11** (a), sodium (Na I) and chlorine (Cl II) were identified in the plasma of 1.9 % NaCl aqueous propellant by comparing acquired emission lines with a standard reference. Additionally, emission lines from neutral and singly ionized oxygen were identified. They were more intensified than using pure water. On the contrary, in the case of 5.5 % NH3 aqueous propellant, spectrum lines attributed from ammonia was not identified as shown in

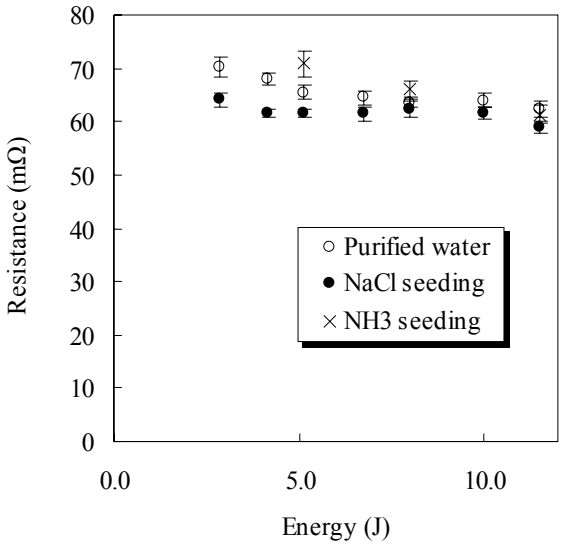

Figure 10. Effect of seeding on the total resistance of the LP-PPT

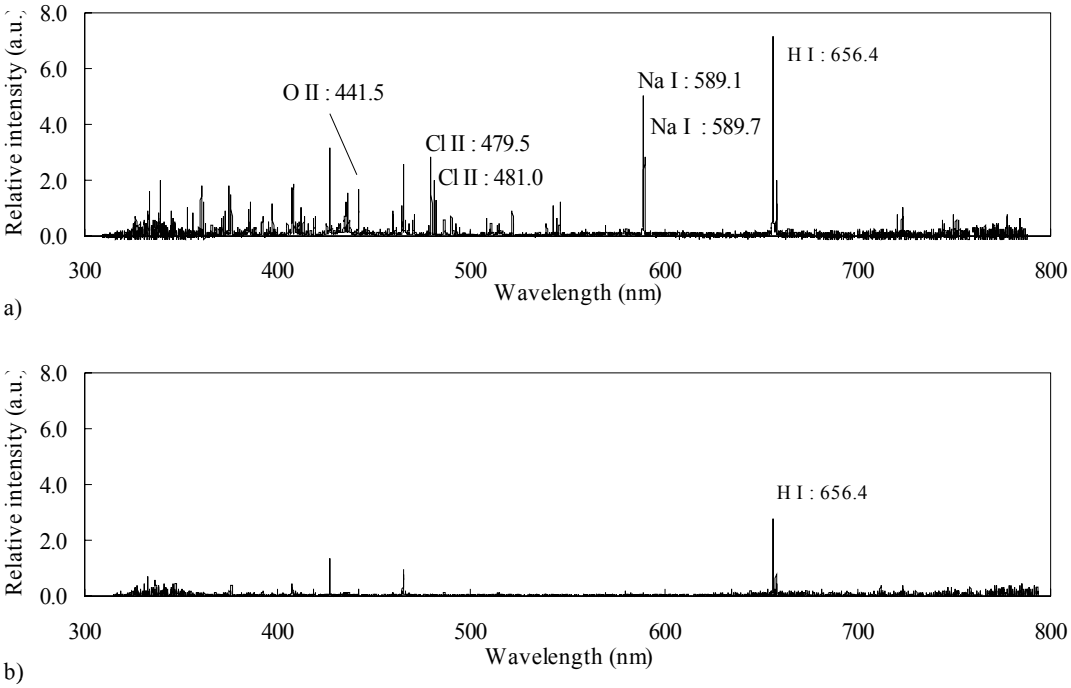

Figure 11. Effect of seeding on the emission spectrogram.
a) NaCl seeding and b) NH_3 seeding

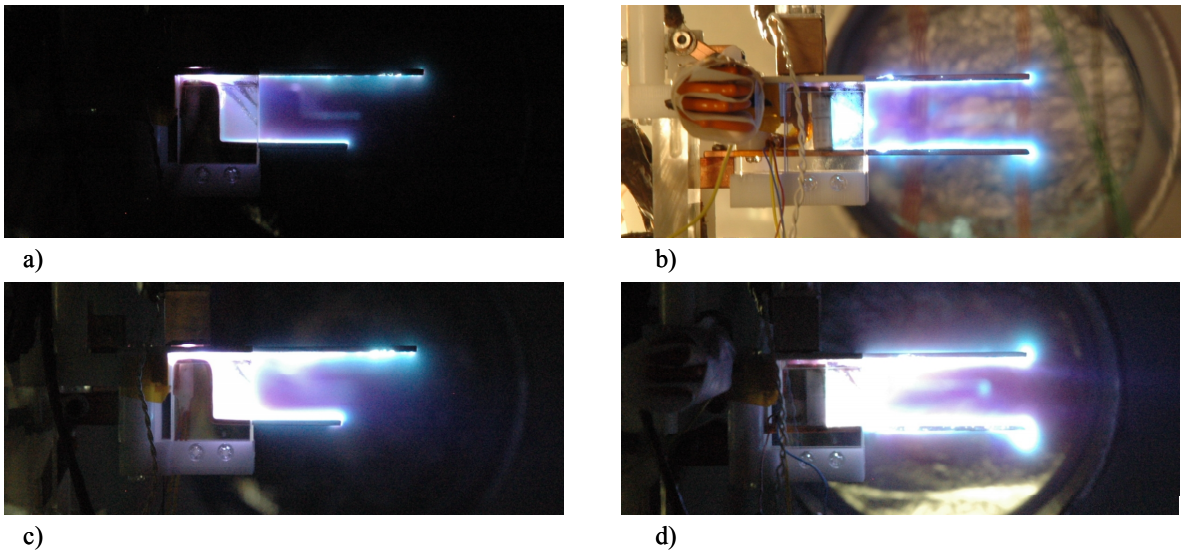

Figure 12. Photographs during the firing of LP-PPT using microheater.
a) Single discharge LP-PPT with close diaphragm, b) double discharge LP-PPT with open diaphragm, c) Single discharge LP-PPT with close diaphragm, and d) double discharge LP-PPT with open diaphragm.

Fig. **11** (b). The overall emission lines became weaker than pure water. This result seems to agree with the result of thrust and resistance measurement.

B. Enhancement of Vaporization Using the Microheater Assembly

1. Operation

Both LP-PPTs using microheater, single discharge and double discharge, were successfully operated with the mass shot over 6 μg keeping the heater temperature at 100 ˚C. By injecting liquid droplets on the microheater, breakdown occurred between electrodes. Figure **12** shows photographs during LP-PPT firing with the exposure time of camera over 200 ms. In double discharge LP-PPT, when the liquid was injected with applying voltage only to the ignition capacitor, small discharge occurred between ignition electrodes.

The ignition characteristics was the same between two LP-PPTs. At the standard temperature around 20 ˚C, there was no breakdown by injecting water droplets of 20μg. Increasing the temperature, the threshold for the reliable ignition was increased and it reached to 6 μg at 100 ˚C. In the mass shot of 4 to 6 μg, the reliable breakdown was not accomplished at the heater temperature of 100 ˚C, that is in several times breakdown did not occur. Under the 4 μg of mass shot, no breakdown occurred.

Figure **13** shows how the threshold changing against the heater temperature and mass shot for another ignition electrode with the electrode length of 25 mm (the others are the same). In that figure, probability means a fraction of number of ignitions over number of trials. The trial number was 15 or 30.

2. Thrust to power ratio

Figure **14** shows the thrust to power ratio, impulse bit per energy, for single and double discharge LP-PPT. Every plot was averaged over 10 single shots measurement and the error bar means the standard

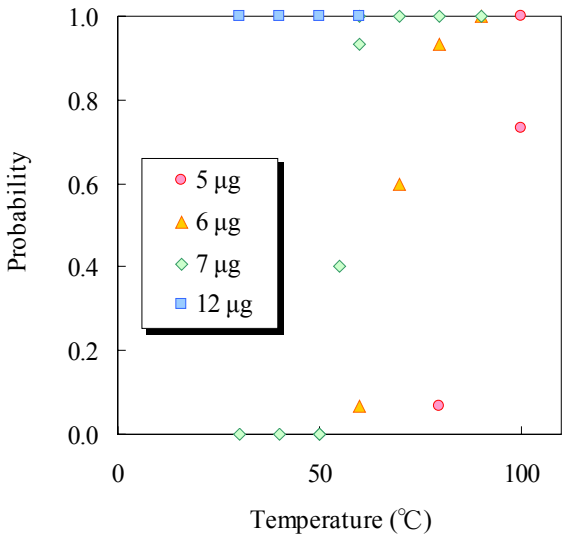

Figure 13. Ignition probability dependence on the heater temperature of the *l* = 25 mm electrode.

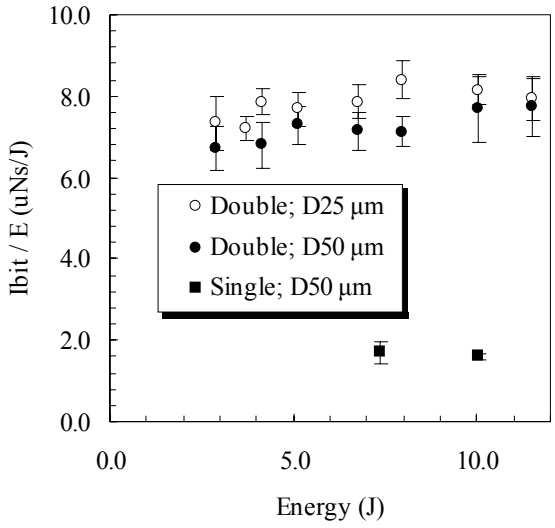

Figure 14. Thrust to power ratio vs. energy in LP-PPT using microheater

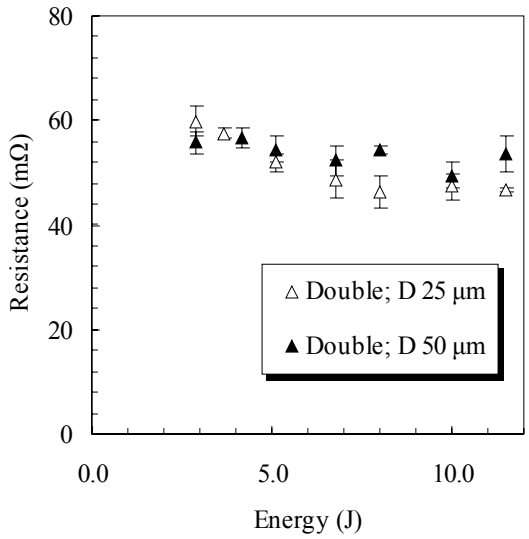

Figure 15. Total resistance vs. energy in double discharge LP-PPT using microheater

deviation. In this experiment the mass shot was kept constant of 6 μg.

Double discharge LP-PPT showed higher thrust to power ratio than the previously studied LP-PPT. The thrust to power ratio was gradually increase with increasing the energy, and saturated around 10 J, where they reaches up to 8 μNs/J. Our previous study had showed the maximum thrust to power ratio of 6 μNs/J. On the other hand, single discharge LP-PPT showed poor thrust to power ratio below 2 μNs/J, which is less than half of the previous LP-PPT.

In addition, the thrust to power was a little increased using small liquid injection orifice. For double discharge LP-PPT, two sizes of liquid injection orifice of 25 and 50 μm were examined.

3. Total resistances

Figure **15** shows the total resistance of double discharge LP-PPT for two sizes of the orifice. These resistances were obtained from the integral of the squared current using Eq. (10). Their energy dependence was investigated. Every plot was averaged over 5 shots and the error bar means the standard deviation.

Theses resistances were consistent with the result of thrust to power ratio. The resistances gradually decreased with increasing the energy, and saturated around 10 J, where they reached down to 50 mΩ. Moreover, the difference in the orifice diameter also consisted with the result of thrust to power. Orifice diameter of 25 μm showed a little smaller resistance than 50 μm. Hence, this difference is meaningful.

VI. Discussion

A. Effect of the Enhancement of Vaporization

It is clear that high thrust to power ratio of double discharge LP-PPT is caused by its low plasma resistance. Moreover this reduction of plasma resistance would be due to the increasing of the interelectrode pressure. From Fig. **13** the breakdown between electrodes are obviously effected by the heater temperature. It means the interelectrode pressure is increased by the heater temperature. In short, the interelectrode pressure is raised up to the point to satisfy Paschen's low. Instead, if we use a spark plug, it means there the interelectrode pressure is always lower than Paschen's breakdown. It is the reason that LP-PPT in the previous research had higher resistance than an ablative PPT and also the reason that the seeding did not have so much effect. In Fig. **16**, the resistances of ablative Teflon PPT (Fig. **2** (b)), LP-PPT with spark plug (Fig. **2** (a)), and double discharge LP-PPT (Fig. **15**(b)) are compared. It is shown that the resistances of double discharge LP-PPT is decreased as low as the Teflon PPT.

As interesting result, the orifice diameter of the injector affected the resistances and performance, whereas, in our previous study, the state of liquid droplets had no influence on the performance. It would be caused by the difference in the diameter of the droplets. The orifice of the diameter of 25 μm provides smaller droplets than 50μm

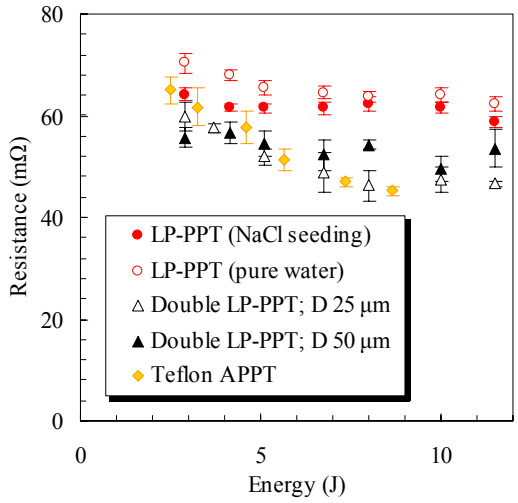

Figure 16. Comparison of total resistances of Teflon PPT, spark plug LP-PPT (pure water and NaCl seeding), and double discharge LP-PPT(the orifice of D25 and D50 μm).

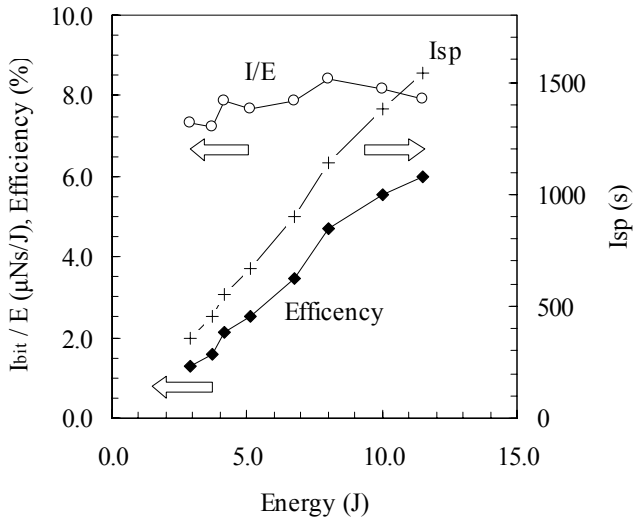

Figure 17.Performance of the double discharge LP-PPT with 25 μm of the orifice.

as shown in images of Fig. **5**. Small droplets on a heater is more rapidly heated and vaporized than lager droplets. This is reason that the injector of the 25 μm orifice provides the higher performance.

B. Effect of the Seeding

Seeding of sodium chloride into water propellant increased the thrust to power ratio by 5 %. This result is consistent with the measured resistance. Considering the result of emission spectroscopy, Seeding of sodium would increase the fractional ionization and electrical conductivity of plasma attributed from water propellant. However, the effect was not so large, and the resistance was still higher than a Teflon PPT. It would be because that, as shown in the experiment of vaporization enhancement using a heater, the cause of the high resistance was its low total number density, rather than the fractional ionization.

Ammonia seeding in water decreased the thrust to power ratio to the contrary. It seems that the plasma density became lower from the weaker emission lines. Some energy might be excessively consumed for the dissociation of ammonia molecule.

C. Performance of the Double Discharge LP-PPT

Figure **17** shows the thruster performance: thrust to power ratio, specific impulse, and thrust efficiency. By increasing the total number density between electrodes, the double discharge LP-PPT had higher thrust to power ratio than LP-PPT with a spark plug by 30 %. On the contrast, the minimum mass shot of the double discharge LP-PPT was raised to 6 μg, which is twice of the previous one. As a result, the specific impulse and thrust efficiency decreases. However, there would not be necessary too high specific impulse, because the liquid propellant does not dominate in the propulsion mass in most of current missions requiring PPTs. Moreover, the decrease of the thrust efficiency is due to the increase of spectrum loss, not decrease of the energy conversion efficiency, which is expressed as follows in PPTs.

$$\eta_{\text{energy}} = \frac{R_{\text{EM}}}{R_{\text{circuit}} + R_{\text{plasma}} + R_{\text{EM}}} \tag{11}$$

To the contrary, in the double discharge LP-PPT, energy conversion efficiency is increased for the decrease of the plasma resistance.

D. Feasibility of an Ignition Capacitor and Microheater Assembly

Feasibility of double discharge LP-PPT is examined as a propulsion system. Double discharge LP-PPT requires an ignition capacitor and a microheater instead of a spark plug. The increment of weight and energy for the ignition capacitor is negligible, because the capacitance is much smaller than main capacitance. In fact the ignition capacitor addressed here consumes the energy of 0.11 J and weighs 25 g.

The microheater addressed here has an enough thermal isolation. Heat conduction through the photoveel circular tube was 110 mW under the 100 K temperature gap. Black body radiation from the heater surface into the space is 90 mW at the heater temperature of 373 K. Hence the total heat loss is 200 mW. This loss would be neglected in a typical operation of 10 J class PPTs. Contrarily, thermal capacity of the microheater assembly has not attained enough level. The main copper body on which the microheater is glued weighs 260 mg, and requires 10 J to heat 100 K gap. It is comparative with the energy per one shot, although, in a long repetitious operation, the initial heating up can be neglected. The capacity would be decreased less than a few Joules by eliminating waste part. The microheater itself, consisted of thin alumina, requires 0.09 J for 100 K heating. The main body needs only the surface to receive liquid droplets. For instance, a circular plate of 2 mm diameter and 0.5 mm thickness is enough size as droplets receiver. Such a plate needs 1.1 J to heat up 100 K.

References

[1] Burton, R. L. and Turchi, P. J., "Pulsed Plasma Thruster," *J. Propul. Power*, Vol. 14, No. 5, 1998, pp. 716-735.

[2] Vondra, R. J., "The MIT Lincoln laboratory PPT," AIAA76-998

[3] Spanjers, G. G., McFall, K. A., Gulczinski III, F. S., and Spores, R. A. "Investigation of Propellant Inefficiencies in a Pulsed Plasma Thruster," *32nd AIAA/ASME/SAE/ASEE Joint Propulsion Conference*, July 1-3, Lake Buena Vista, 1996.

[4] Mikellides, P. G. and Turchi, P. J., "Modeling of Late-time Ablation in Teflon Pulsed Plasma Thrusters," *32nd AIAA/ASME/SAE/ASEE Joint Propulsion Conference*, July 1-3, Lake Buena Vista, 1996.

[5] Spanjers, G. G., Lotspeich, J. S., McFall, K. A., and Spores, A., "Propellant Losses Because of Particulate Emission in a Pulsed Plasma Thruster," *J. Propulsion Power*, Vol. 14, No. 4, 1998, pp. 554-559.

[6] Aston, G and Pless, C., "Ignitor Plug Operation in a Pulsed Plasma Thruster," *J. Spacecraft*, Vol. 19, No.3, 1982, pp. 250-256.

[7] Palumbo, D. J. and Guman, W. J., "Effects of Propellant and Electrode Geometry on Pulsed Ablative Plasma Thruster Performance," *J. Spacecraft*, Vol. 13, No. 3, 1976, pp. 163-167.

[8] Gluczinski, F., Dulligan, M., Lake, J., and Spangers, G. G., "Micropropulsion Research at AFRL," *36th AIAA/ASME/SAE/ASEE Joint Propulsion Conference*, 16-19 July, Huntsville, Alabama, 2000.

[9] Keidar, M. and Boyd, D. I., "Analysis of Teflon Surface Charring and near field plume of a Micro-Pulsed Plasma Thruster," *27th International Electric Propulsion Conference*, October 15- 19, Pasadena, California, 2001.

[10] Takegahara, H., Igarashi, M., Kumagai, N., Sato, K., and Tamura, K., "Evaluation of Pulsed Plasma Thruster System for μ-Lab Sat II," *27th International Electric Propulsion Conference*, October 15-19, Pasadena, California, 2001.

[11] Kakami, A., Koizumi, H., Komurasaki, K., and Arakawa, Y., "Preliminary Study on Liquid Propellant PPT," *27th International Electric Propulsion Conference*, Pasadena California, America, Poster Session, Oct. 2001.

[12] Kakami, A., Koizumi, H., Komurasaki, K., and Arakawa, Y., "Liquid Propellant PPT Performance," *Proceedings of the 23rd International Symposium on Space Technology and Science*, Vol. 1, 2002, pp. 307-312.

[13] Koizumi, H., Kakami, A., Furuta, Y., Komurasaki, K., and Arakawa, Y., "Liquid Propellant Pulsed Plasma Thruster," *28th International Electric Propulsion Conference*, March 17-21, 2003, Toulouse, France.

[14] Kakami, A., Koizumi, K., Komurasaki, K., and Arakawa, Y., "Design and performance of liquid propellant pulsed plasma thruster," *Vacuum*, Vol. 73, 2004, pp.419-425.

[15] Scharlemann, C. A. and York, T. M., "Investigation of a PPT Utilizing Water as Component Propellant," *28th International Electric Propulsion Conference*, March 17-21, 2003, Toulouse, France.

[16] Simon, D. H. and Land, H. B., "Micro Pulsed Plasma Thruster Technology Development," *40th AIAA/ASME/SAE/ASEE Joint Propulsion Conference*, Fort Lauderdale, Florida, July 11-14, 2004.

[17] Jahn, R., G., *Physics of Electric Propulsion*, McGraw-Hill, New York, 1968, Chaps. 9.

[18] Koizumi, H., Furuta, Y., Komurasaki, K., and Arakawa, Y., "A Pulsed Plasma Thruster Using Water as the Propellant," *40th AIAA/ASME/SAE/ASEE Joint Propulsion Conference*, Fort Lauderdale, Florida, July 11-14, 2004.

[19] Cambel, A. B., *Plasma Physics and Magnetofluidmechanics*, McGraw-Hill, New York, 1963, Chaps. 7, 14.

[20] Anderson, H. L. (ed.), *Pysics Vade Mecum*, American Institute of Physics, New York, 1981.

[21] Koizumi, H., Komurasaki, K., and Arakawa, Y., "Development of Thrust Stand for Low Impulse Measurement from Microthrusters," *Rev. Sci. Instrum.* Vol. 75, No. 10, 2004, pp.3185-3189.